33rd Annual International Conference of the IEEE EMBS
Boston, Massachusetts USA, August 30 - September 3, 2011

Experimental Characterization of Intrapulse Tissue Conductivity Changes for Electroporation

Robert E. Neal II, Paulo A. Garcia, John L. Robertson, and Rafael V. Davalos, *Member, IEEE*

***Abstract*—Cells exposed to short electric pulses experience a change in their transmembrane potential, which can lead to increased membrane permeability of the cell. When the energy of the pulses surpasses a threshold, the cell dies in a non-thermal manner known as irreversible electroporation (IRE). IRE has shown promise in the focal ablation of pathologic tissues. Its non-thermal mechanism spares sensitive structures and facilitates rapid lesion resolution. IRE effects depend on the electric field distribution, which can be predicted with numerical modeling. When the cells become permeabilized, the bulk tissue properties change, affecting this distribution. For IRE to become a reliable and successful treatment of diseased tissues, robust predictive treatment planning methods must be developed. It is vital to understand the changes in tissue properties undergoing the electric pulses to improve numerical models and predict treatment volumes. We report on the experimental characterization of these changes for kidney tissue. Tissue samples were pulsed between plate electrodes while intrapulse voltage and current data were measured to determine the conductivity of the tissue during the pulse. Conductivity was then established as a function of the electric field to which the tissue is exposed. This conductivity curve was used in a numerical model to demonstrate the impact of accounting for these changes when modeling electric field distributions to develop treatment plans.**

I. Introduction

Irreversible electroporation (IRE) is a non-thermal focal ablation technique that uses minimally invasive electrodes to deliver brief electric pulses to tissue. This external electric field alters the transmembrane potential on the cell's lipid bilayer. Depending on the energy of the pulses, there can be no macro-effect on the integrity of the bilayer, or nano-scale defects may be formed in a process known as electroporation. When the energy of the pulses is high enough, these defects are irrecoverable and kill the cell in a non-thermal manner. IREs unique mechanism spares the extracellular matrix and preserves major vasculature and other sensitive structures[1-3]. Treatments are predictable with numerical modeling[4], and resolve rapidly[1] with sub-millimeter resolution between treated and unaffected cells[5]. Treatments promote an immune response, are unaltered by blood flow, may be administered quickly (~5min), and can be visualized in real-time[1, 6-8].

The effects of IRE therapy on tissue are related to the electric field distribution within the tissue[4], which is dependent on the physical characteristics of the tissue and electrodes, the pulse parameters used, and the electrical conductivity of the tissue. One effect of creating the defects in the cell membrane is improved electrolyte mobility across the membrane, which can significantly alter the bulk conductivity of the affected regions of tissue. In addition, tissue conductivity increases with temperature. The electric pulses in electroporation therapies will cause tissue heating due to Joule heating from bulk tissue resistance. These two factors will influence the electric field distribution that the tissue experiences, and therefore the treatment region[9-11].

Successfully implementing IRE and other electroporation-based therapies requires the ability to reliably predict the affected volume for treatment planning. This can be done with numerical modeling to solve for electric field distributions. To improve the accuracy of these numerical models, tissue property changes from electroporation therapies must be characterized and accounted for.

It has been shown previously that bulk tissue properties will change in response to temperature changes[12] as well as electroporation[13, 14]. It has been suggested to harness this phenomenon as a method for monitoring electroporation therapy effects in real-time[15]. Here, we present the results of experimental characterization of the intra-pulse effects on tissue conductivity when subjected to typical IRE electric pulses over a range of electric fields. A simple model demonstrates how the electric field distribution changes when accounting for these effects. Porcine kidney tissue samples were pulsed while simultaneously recording the voltage and current data in real-time. This was repeated for electric fields ranging from 200-2000 V/cm, and increases in conductivity were observed as a function of electric field as well as pulse duration.

II. Methods

A. Experimental Setup

The medulla of kidneys contains the collecting system and ureter for the organ, which will present a great deal of heterogeneities and possibly affect experimental results[10, 16]. However, the bulk properties of the cortex are relatively homogeneous and suitable for characterizing the bulk changes resulting from the electric pulses.

Tissue samples were collected from porcine kidneys

Manuscript received April 15, 2011. This work was supported in part by The Coulter Foundation.

R. E. Neal II, P. A. Garcia, and R. V. Davalos are with the Bioelectromechanical Systems Laboratory in the Virginia Tech-Wake Forest School of Biomedical Engineering and Sciences, Virginia Tech, Blacksburg, VA 24060 (phone: 540-231-1979, fax: 540-541-8320, e-mail: nealre@vt.edu, pgarcia@vt.edu, davalos@vt.edu).

J. Robertson is with the Virginia-Maryland School of Veterinary Medicine at Virginia Tech, Blacksburg, VA 24060 USA (e-mail: drbob@vt.edu).

harvested within 15 minutes post-mortem. Kidneys were sectioned into flat cores approximately 5 mm thick and 8 mm in diameter. Sample dimensions were measured with calipers, and the sample was placed between two plate electrodes with 0.7 mm diameter holes to allow access for a fluoroptic thermometer (LumaSense Technologies, Santa Clara, CA). Numerical modeling showed the electric field losses on the tissue from the hole were less than 1% over the tissue volume (data not shown). All experimental trials were completed within 2 hours post-mortem.

Homogeneous tissue samples placed entirely between plate electrodes result in electric fields equal to voltage divided by distance. Voltages were delivered to generate electric fields ranging between 200-2000 V/cm over a pulse duration of 500 µs, a pulse length long enough to encompass common IRE and electrochemotherapy protocols.

Electric pulses were delivered using the ECM830 pulse generator, and voltage was measured using the Enhancer 3000 Monitoring System (both Harvard Apparatus, Cambridge, MA). In addition, a low impedance (0.1 Ohm) voltage divider was used with a separate circuit using an INA128 op-amp to measure the current from the pulses. Both the voltage and current measuring circuits were run to a two channel oscilloscope (Tektronix, Beaverton, OR) with an adjustable trigger for capturing the pulses.

Matlab software was used to collect the captured pulse data from the oscilloscope for the voltage and current at a sampling rate of 1 MHz (Mathworks, Natick, MA). A function was written to smooth the data with 25 and 10 point moving averages for current and voltage data, respectively. It sets the data baseline average to zero and coordinates identical initial time points for the voltage and current data onset to ensure synchronization. The conductivity was solved for the entirety of the pulse according to the equation:

$$\sigma(t) = \frac{i(t) \cdot d}{V(t) \cdot SA} \quad (1)$$

where σ(t) is the conductivity of the tissue, *i(t)* is the current, *V(t)* is the voltage, *d* is the separation distance between the plates, and *SA* is the cross sectional area of the tissue.

B. Numerical Model

The conductivity was solved throughout the entire pulse for each electric field examined. The resulting data was used to develop an equation for conductivity as a function of electric field strength and time. This conductivity function has been applied to a simple numerical model simulation to demonstrate how accounting for the changes in conductivity found experimentally will affect the modeled electric field distribution, and therefore treatment region.

The numerical model was created using finite element modeling software (Comsol Multiphysics, Stockholm, Sweden). The tissue domain is composed of a homogeneous sphere 10 cm in diameter with an initial electrical conductivity taken from the literature of 0.15 S/m[17]. Two needle electrodes each 1 mm in diameter, 1 cm long, and separated by 2 cm, were placed in the center of the domain, which was large enough to prevent any observable boundary effects on the model results. The electric field distribution was solved for using the Laplace equation

$$\nabla \cdot (\sigma \nabla \Phi) = 0$$

where σ is the electrical conductivity of the tissue and Φ is the electric potential. The tissue boundary was set as electrically insulating, while 1 electrode was set to V_o = 2000 V and the other to ground. The short pulse durations used in the single pulse experiments resulted in negligible temperature changes as measured by the fluoroptic thermometer, and thermal effects on the model have therefore been excluded (data not shown). The model was solved for two conditions, one in which the tissue's conductivity remains constant at its baseline level, and one that uses the conductivity curve developed from the experiments.

III. Results

A. Experimental Results

Experiments were performed continuously for an identical voltage over 2 hours and no discernable trend in tissue conductivity based on time post-mortem was observed (data not shown).

Representative voltage and current curves may be seen in Fig. 1. From here, one can see how the sudden rise in the voltage due to its square waveform initially introduces large fluctuations in the current, which soon settle once the voltage has reached its plateau value.

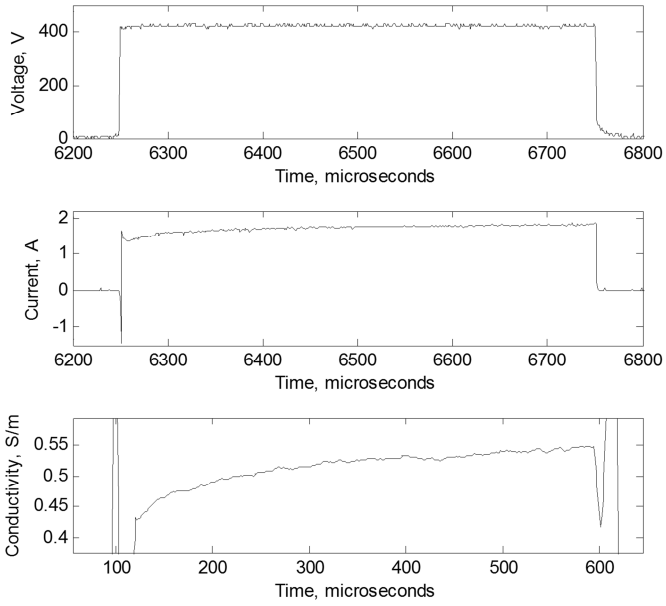

Fig. 1. Waveforms for voltage, current, and conductivity from a 500 µs pulse at 800 V/cm.

It should be noted for Fig. 1 that recording started prior to pulse delivery, so the time scale for voltage and current is

offset by ~6.25 seconds. This has been adjusted for in the conductivity plot, where all data has been trimmed beyond 100 data points prior to and after completion of the pulse.

Calculations were conducted for 200, 500, 1000, and 2000 V/cm, each at n = 6. From these data, average conductivities were calculated throughout the pulse. To eliminate variability from the rapid fluctuations at the beginning and end of the pulses, the rise and decay times from the voltage were eliminated to extract only the conductivity values after initial voltage and current settling. A plot of all averaged data may be found in Fig. 2.

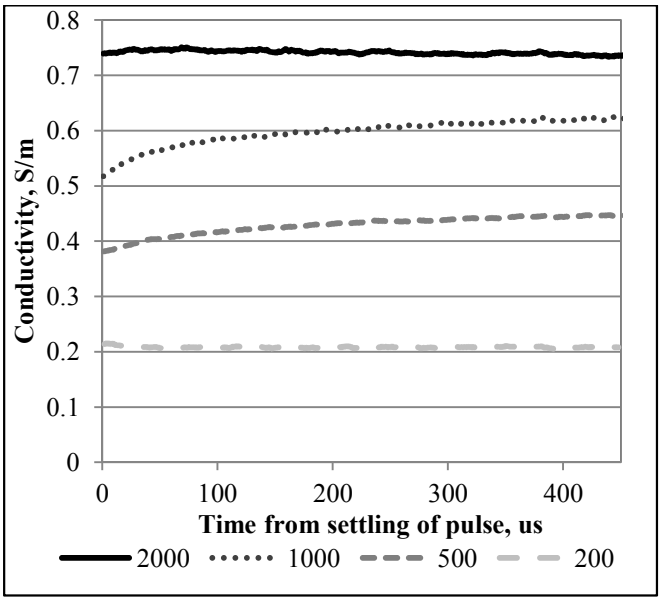

Fig. 2. Conductivity v. time for 4 electric field distributions.

B. Numerical Model

The numerical model setup may be seen in Fig. 3A. This model was solved for two conditions. The baseline conductivity for the model was taken from the literature, since 200 V/cm was the lowest electric field distribution that we could reliably acquire the current and voltage data with our system, and an increase above the literature values was already observable at this point.

For the first case, the baseline electric field distribution for a homogeneous conductivity volume is depicted with isocontours representing regions of reversible and irreversible electroporation taken from the literature[4, 18]. For the second case, the baseline electric field distribution was taken to determine the conductivity. This was done by fitting the initial conductivities from the investigated electric fields to fit a conductivity curve as a function of electric field based on the measured conductivities at 100 µs. The resulting conductivity map may be seen in Fig. 3B. The final distribution of predicted areas for reversible and irreversible electroporation may be seen in Fig. 3D, where it can clearly be seen that the size of the affected region changes.

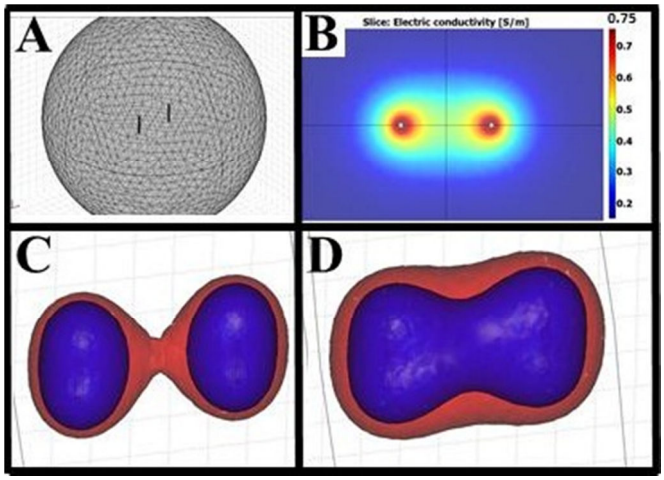

Fig. 3. Numerical Simulation Results. (A) Numerical model setup where two needle electrodes are inside a sphere of tissue. (B) Conductivity map from for σ(E). (C) Electric field contours of 350 and 500 V/cm for 2000 V applied in homogeneous tissue. (D) Identical electric field contours with experimentally derived conductivity changes.

IV. Discussion

This study provides insight into the behavior of tissue when subjected to short, square wave electric pulses of typical electroporation protocols. There is a clear, nearly immediate change in tissue conductivity based on the electric field to which it is exposed. Furthermore, depending on the presence of continued permeabilization, either by increasing the number of pores or individual pore size, this conductivity continues to increase with time, which can be seen for the 500 and 1000 V/cm trials. Although the tissue experiences Joule heating during this time, experimental measurements and numerical modeling of the temperature showed that the temperature-based conductivity increases were negligible relative to those observed during the pulse. This is because temperature change within such a short, single pulse is small. Therefore, another mechanism for the continued increase in conductivity must be considered.

When the pores in a cell are opened, there is a sudden increase in electrolyte mobility across the lipid membrane. This will reduce the membrane's dielectric properties, rapidly reducing the transmembrane potential. Therefore, for conductivity to increase beyond the initial permeabilization, the external electric field to which the tissue is exposed must be high enough to keep an adequate transmembrane potential that will continue to result in increased membrane defects, or size of these defects. The 200 V/cm group did not increase over time, suggesting that either there was no pore formation or that the electric field was not able to overcome the membrane's ability to neutralize its transmembrane potential, mitigating any progression of pore formation.

It is interesting to observe that the increase in conductivity with electric field appears to plateau at 2000 V/cm, where a maximum conductivity appears to have been encountered. This may be due to the inherent properties of the tissue.

Biological fluids such as blood and interstitial fluid have a conductivities ranging between 0.8-1.9 S/m[12]. Therefore, a tissue composed entirely of such fluid would have this value as an absolute maximum that the conductivity can reach. For pulse lengths of typical electroporation protocols, the membrane initially behaves as a dielectric, and electrolytes must flow around the cells through the interstitial and other biological fluids. This leads to the initial lower conductivity for the tissue. Once the cells become permeabilized, ions can flow directly through the cells, resulting in the increased tissue conductivity observed from our experimental investigation. However, even if all of the cells have become completely permeabilized, inherent resistance from support structures such as the extracellular matrix will dominate resistance in the tissue. It is possible that these structures induce the inherent plateau for electrical conductivity in the tissue, and explains why it is below the conductivity of pure isotonic fluids. Future work will investigate the approach of this plateau with higher resolution electric field data.

It is important to note that in addition to size, the shape of the electric field distribution also changes when accounting for conductivity changes. This effect is important for planning treatment protocols in the vicinity of sensitive structures such as blood vessels and nerves, where the resulting increase in electric field into these larger volumes will also result in increased Joule heating. Joule heating in tissue is defined as $\sigma|\nabla\Phi|^2$. Therefore, it can be seen that increasing the conductivity and the electric field in the region will result in substantially different thermal effects. Many of IREs benefits, including minimal scar formation, sparing of supporting and sensitive structures, and rapid lesion resolution are a result of its unique non-thermal mechanism for cell destruction. If appropriate caution is not taken to ensure that the affected regions are not subjected to significant thermal damage, then many of IREs advantages may be compromised and complications similar to thermal therapies may arise. Future experimental validation of treatment volumes will be vital to further refining simulation techniques. As improved models become validated, their effects may be incorporated into clinical treatment planning software which would enable physicians to readily adjust treatment protocols until the entirety of a targeted volume is treated while sparing as much healthy tissue as possible.

V. Conclusion

This study characterized the effects of electric pulses on the conductivity of kidney tissue as a function of electric field and time. It was found that initial increases in conductivity occur almost instantaneously based on the electric field. For higher fields, transient increases in conductivity are experienced over the length of the pulse. The highest electric field examined suggests a plateau in conductivity, where all cells become permeabilized and conductivity no longer increases with time, except as a function of temperature. Numerical models created to incorporate this change in electrical conductivity demonstrate a significant increase in tissue volume exposed to a given electric field and a changed distribution shape. Applying improved models to treatment planning should enable physicians to more accurately plan and implement therapeutic IRE and other electroporation based therapies.

Acknowledgment

This work supported by The Coulter Foundation and The National Science Foundation Grant NSF CBET-093335. The authors acknowledge Chris Arena, Mike Sano, and John Caldwell for their assistance with the instrumentation.

References

[1] G. Onik, *et al.*, "Irreversible Electroporation: Implications for Prostate Ablation," *Technol Cancer Res Treat,* vol. 6, pp. 295-300, 2007.

[2] E. Maor, *et al.*, "The Effect of Irreversible Electroporation on Blood Vessels," *Technol Cancer Res Treat,* vol. 6, pp. 307-312, 2007.

[3] K. Thomson, "Human Experience with Irreversible Electroporation," in *Irreversible Electroporation*, B. Rubinsky, Ed., ed Heidelberg: Springer Berlin, 2010, pp. 249-254.

[4] D. Miklavcic, *et al.*, "A validated model of in vivo electric field distribution in tissues for electrochemotherapy and for DNA electrotransfer for gene therapy," *Biochimica et Biophysica Acta,* vol. 1523, pp. 73-83, 2000.

[5] J. F. Edd, *et al.*, "*In Vivo* Results of a New Focal Tissue Ablation Technique: Irreversible Electroporation," *IEEE Trans Biomed Eng,* vol. 53, pp. 1409-1415, 2006.

[6] E. W. Lee, *et al.*, "Imaging Guided Percutaneous Irreversible Electroporation: Ultrasound and Immunohistological Correlation," *Tech Cancer Res Treat,* vol. 6, pp. 287-293, 2007.

[7] L. M. Mir and S. Orlowski, "Mechanisms of electrochemotherapy," *Adv Drug Deliv Rev,* vol. 35, pp. 107-118, 1999.

[8] B. Rubinsky, *et al.*, "Irreversible Electroporation: A New Ablation Modality - Clinical Implications," *Technol Cancer Res Treat,* vol. 6, pp. 37-48, 2007.

[9] N. Pavselj, *et al.*, "The course of tissue permeabilization studied on a mathematical model of a subcutaneous tumor in small animals," *Biomedical Engineering, IEEE Transactions on,* vol. 52, pp. 1373-1381, 2005.

[10] R. E. Neal, 2nd and R. V. Davalos, "The Feasibility of Irreversible Electroporation for the Treatment of Breast Cancer and Other Heterogeneous Systems," *Ann Biomed Eng,* vol. 37, pp. 2615-2625, 2009.

[11] J. F. Edd and R. V. Davalos, "Mathematical Modeling of Irreversible Electroporation for Treatment Planning," *Technol Cancer Res Treat,* vol. 6, pp. 275-286, 2007.

[12] F. A. Duck, *Physical Properties of Tissue: A Comprehensive Reference Book*. New York: Academic Press, 1990.

[13] A. Ivorra, *et al.*, "In vivo electrical conductivity measurements during and after tumor electroporation: conductivity changes reflect the treatment outcome," *Phys Med Biol.,* vol. 54, pp. 5949-63. Epub 2009 Sep 17., 2009.

[14] A. Ivorra and B. Rubinsky, "In vivo electrical impedance measurements during and after electroporation of rat liver," *Bioelectrochemistry.,* vol. 70, pp. 287-95. Epub 2006 Oct 21., 2007.

[15] R. V. Davalos, *et al.*, "Electrical impedance tomography for imaging tissue electroporation," *Biomedical Engineering, IEEE Transactions on,* vol. 51, pp. 761-767, 2004.

[16] C. Daniels and B. Rubinsky, "Electrical Field and Temperature Model of Nonthermal Irreversible Electroporation in Heterogeneous Tissues," *J Biomech Eng,* vol. 131, p. 071006, 2009.

[17] T. W. Athey, *et al.*, "Measurement of Radio Frequency Permittivity of Biological Tissues with an Open-Ended Coaxial Line: Part I," *Microwave Theory and Techniques, IEEE Transactions on,* vol. 30, pp. 82-86, 1982.

[18] P. Garcia, *et al.*, "Intracranial Nonthermal Irreversible Electroporation: In Vivo Analysis," *J Membr Biol,* vol. 236, pp. 127-136, 2010.